On the Design of Pulse Detonation Engines

T.W. Chao, E. Wintenberger, J.E. Shepherd
Graduate Aeronautical Laboratories
California Institute of Technology
Pasadena, CA 91125
U.S.A.

GALCIT Report FM 00-7

Prepared for General Electric, contract GE-PO A02 81655
under DABT-63-0-0001

January 15, 2001

Abstract

This report addresses some basic issues in the structural and performance aspects of Pulse Detonation Engines (PDEs). Performance parameters studied include thrust-specific-fuel-consumption (TSFC), frequency limits, and thrust-to-weight ratio. A design surface is developed that accounts for various design limits. The structural aspects deal with critical parameters, material properties, and phenomena such as engine geometry, mass, yield stress, structural resonance due to flexural wave excitation, critical flaw size, and fracture toughness. Four materials for PDEs were chosen for comparison: silicon nitride, inconel, steel, and aluminum. Estimates of wall thickness and thrust-to-weight ratio are given over a range of operating conditions. Key issues and areas for further work are identified for both propulsion and performance aspects.

Contents

List of Figures

List of Tables

1 Introduction

In this study, we consider the conceptual design of a pulse detonation engine with a thrust of about 100 N and a tube diameter in the range of 1 to 2 inches. The design parameters and targets for this study are summarized in Table 1:

Parameter	Goal
Thrust	100 N
Frequencies	100 Hz - 200 Hz
Mixture	Stoichiometric JP10-air
Initial conditions	100 kPa and 300 K
Tube diameter	2.5 - 5 cm
Engine weight	<1.2 kg
Thrust-to-(engine) weight ratio	>8
Thrust-specific-fuel-consumption (TSFC)	>0.15 (kg/hr)/N

Table 1: Design parameters and goals

The goal of the present study is to estimate in a very simple fashion some of the critical parameters of a pulse detonation engine in this size range. While our estimates are based on sound engineering principles and data, our engine model is very naive. We have not considered important aspects such as inlet diffusers, air valves, fuel injection and mixing, exhaust nozzles or flight path effects. All of these factors will be significant in real applications. However, important trends and figures of merit can be obtained from these analyses.

The analysis is divided into two portions. First, the propulsion performance is predicted using the properties of JP10 detonation and a simple model of a single cycle. Second, the choice of tube materials and dimensions is considered using ideas from strength of the materials and fracture mechanics. We conclude with a discussion of important material properties issues that we have not considered.

2 Performance considerations

The pulse detonation engine will be operated with a stoichiometric JP10-air mixture at ambient conditions ($P_1 = 100$ kPa and $T_1 = 300$ K). The detonation properties of JP10 ($C_{10}H_{16}$) are summarized in Table 2. The propulsion performance is estimated on the basis of an idealized single-cycle operation, described below.

2.1 Detonation physics of a single-cycle pulse detonation engine

A pulse detonation engine repeats the same cycle up to several hundred times per second. A single cycle consists of four major steps: 1) filling of the tube with the desired mixture; 2) detonation initiation; 3) propagation of the detonation along the tube; 4) exhaust of the

Initial density of mixture	$\rho_\circ$	1.221	kg/m^3
Mole fraction of fuel	Y_f	0.01478	
Mass fraction of fuel	X_f	0.066168	
Chapman-Jouguet pressure	P_{CJ}	1.84	MPa
Chapman Jouguet velocity	U_{CJ}	1783.5	m/s
Stationary products thrust pressure	ΔP_3	0.585	MPa
Stationary products sound speed	c_3	914.9	m/s
Mixture-based specific impulse	I_{sp}	114.6	s
Impulse per unit volume	I_v	1372.5	N·s/m^3
Cell width	λ	60	mm

Table 2: JP10 detonation properties.

products to the atmosphere (see Figure 1). A detonation wave is a supersonic combustion wave consisting of a shock wave coupled with a reaction zone. The conditions behind an ideal detonation wave are dictated by the Chapman-Jouguet (CJ) condition that the flow behind the wave be sonic in a reference frame moving with the detonation velocity.

A detonation wave, therefore, propagates at a unique velocity U_{CJ}, which is a function of the mixture composition and the initial thermodynamic conditions. This velocity and other properties such as the pressure P_{CJ} behind the detonation wave can be computed given the thermodynamic properties of the initial mixture and the products. This is how the values given in Table 2 were obtained. Laboratory experiments have validated these estimations for detonation wave velocity and pressure, impulse measurements are in progress for JP10.

For an ideal situation, the initiation process takes only a short time and the detonation wave is quickly established, propagating near the CJ velocity. A detonation wave propagating in a closed-end tube is followed by an isentropic expansion wave (Taylor wave) that brings the flow to rest at some distance behind the detonation wave. The pressure decreases to a value of P_3 at the closed end of the tube while the detonation is propagating and for a short period of time afterwards. When the detonation reaches the open end of the tube, the detonation process ceases since there is no fuel outside the tube. The detonation products flow out of the tube, creating a shock wave in the external region and a series of expansion waves[1] are reflected back into the tube. As the tube is emptied, the pressure decreases to equal the ambient value, often with an intermediate excursion to subambient values.

For the purposes of estimating impulse, only the pressure at the closed end of the tube must be known. The thrust or force on the tube can be found by integrating the pressure over the area of the end wall. As discussed by Wintenberger et al. (2000), the pressure on the thrust wall consists of a negligible excursion to the Chapman-Jouguet pressure peak P_{CJ}, a constant pressure P_3 regime, and decreasing pressure associated with the exhaust process. An idealized schematic of this pressure history is shown in

[1]For hydrocarbon fuels, the reflected wave is always an expansion but compression waves can also be created in certain cases with hydrogen as the fuel.

Figure 2.

The simplest way to characterize the performance of an ideal cycle is to integrate the thrust over the duration of the cycle to obtain the impulse. This computation was carried out in Wintenberger et al. (2000) using the model thrust wall pressure history described above. The resulting impulse can be expressed in at least two ways: 1) impulse per unit volume I_v and 2) impulse per unit mass or specific impulse I_{sp}. The impulse per unit volume is independent of the tube size and very useful in design studies. The impulse per unit volume is directly proportional to the plateau pressure P_3 and inversely proportional to the detonation velocity (Wintenberger et al., 2000)

$$I_v = \Delta P_3 \left[\frac{1}{U_{CJ}} + (\alpha + \beta) \frac{1}{c_3} \right] \tag{1}$$

where α and β are two non-dimensional parameters characteristic of the constant and decaying parts of the pressure signal (estimated in Wintenberger et al. 2000); ΔP_3 and c_3 are the overpressure and sound speed of the products after the Taylor wave.

The specific impulse is commonly used as a figure of merit in the propulsion community and is defined as

$$I_{sp} = \frac{I_v}{g_\circ \rho} \tag{2}$$

where $g_\circ$ is the standard acceleration due to earth's gravity (9.81 $\mathrm{m{\cdot}s^{-2}}$) and ρ is the initial mixture mass density.[2] This definition is the direct analogue of that used in rocket motor performance evaluation. The advantage of specific impulse as a figure of merit is that it is relatively independent of initial pressure (as long as it is sufficiently high) whereas impulse per unit volume scales directly with initial pressure, all other factors being the same. The values of c_3 and P_3 can be calculated from the CJ values using isentropic flow conditions (Table 2). The impulse estimated in this fashion has been compared (Wintenberger et al., 2000) to measured values for several hydrocarbon fuels (C_2H_2, C_2H_4, C_3H_8) and hydrogen in oxygen-nitrogen mixtures. Measured and estimated values are within 10% for most cases in which the detonation is promptly initiated.

2.2 Geometry

This design study assumes that the detonation tube has constant diameter along the length of the tube. There are three geometrical parameters that can be varied: the diameter of the tube d, the length of the tube L and the cycle repetition frequency f. The mixture considered in the present study has an impulse per unit volume: $I_v = 1372.5$ $\mathrm{Ns/m^3}$ (Wintenberger et al., 2000). The single-cycle impulse is the product of the impulse per unit volume by the volume of the tube V. The actual thrust T is then calculated by

[2] Some authors use the partial mass density associated with the fuel only rather than the mixture mass density in defining specific impulse. The partial density of the fuel is simply the fuel mass fraction times the total density, so that the value of $I_{sp,fuel} = I_{sp}/Y_f = 775$ s for a stoichiometric JP10–air mixture.

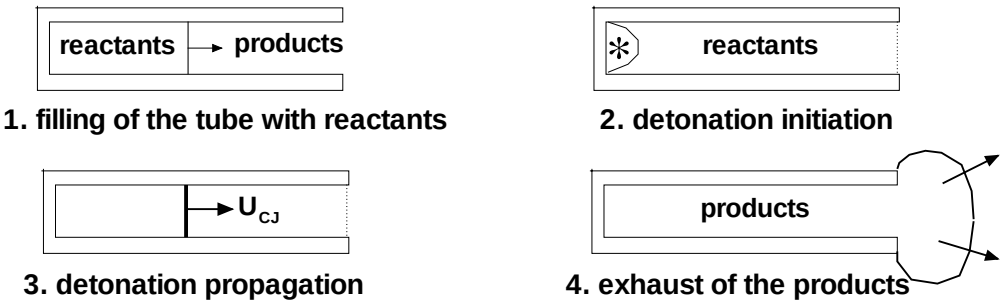

Figure 1: Major steps of an idealized pulse detonation engine cycle.

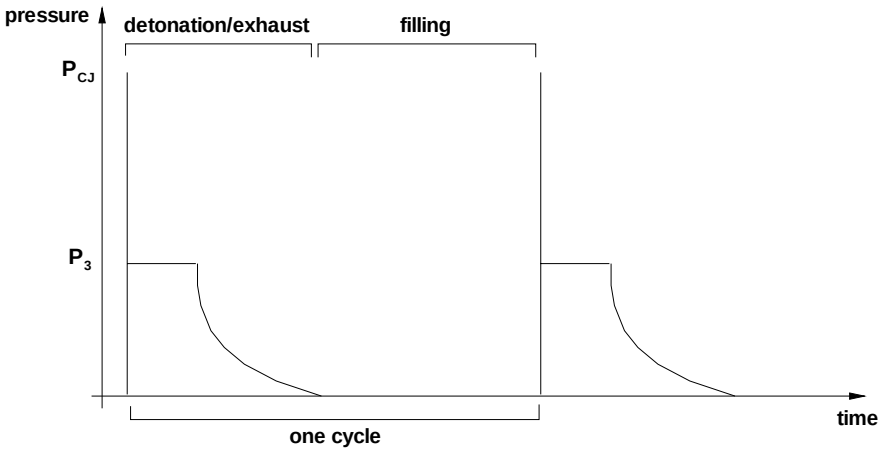

Figure 2: Modelling of a pulse detonation engine cycle. Pressure shown is measured at the thrust wall on far left-hand side of tube shown in Figure 1.

multiplying the single-cycle impulse by the repetition frequency.

$$T = I_v V f = I_v \frac{\pi L d^2}{4} f \tag{3}$$

For a fixed value of thrust, this provides a constraining relationship between the dimensions of the tube and the cycle frequency. For example, the tube length can be expressed as a function of the tube diameter and the cycle frequency. This relationship is plotted in Figure 3.

2.3 Thrust-specific fuel consumption

A figure of merit used in air-breathing propulsion is thrust-specific fuel consumption (TSFC) defined as the fuel mass flow rate divided by the thrust. It represents how much fuel is required to create one unit of thrust. For a pulse detonation engine, this is

$$TSFC = \frac{f Y_f \rho_\circ V}{f I_v V} = \frac{Y_f \rho_\circ}{I_v} \tag{4}$$

Note that in this simple model, the TSFC is independent of the volume and the repetition frequency, since both the thrust and the fuel mass flow rate are proportional to the product of volume and frequency. The fuel partial mass density is equal to the product of the mixture density $\rho_\circ$ and the fuel mass fraction Y_f. For stoichiometric JP10–air, the values of the mixture density $\rho_\circ$ and the fuel mass fraction Y_f are respectively 1.221 kg/m^3 and 0.0662. The value obtained for the TSFC is 0.212 kg/N·hr. It is in the same range as ramjets (for a Mach number of 2) which have a TSFC of the order of 0.17–0.26 kg/N·hr, according to Hill and Peterson (1992).

2.4 Frequency limit

The cycle repetition frequency depends primarily on the length L of the tube. Because the thrust is directly proportional to frequency (see Eq. 3), it is important to estimate the maximum possible frequency at which the engine can be operated. This is the frequency that we will suppose the engine is actually operated at in order to obtain maximum thrust for a given volume.

The upper limit for the cycle repetition frequency f_{max} corresponds to a minimum cycle time t_{cycle}

$$f_{max} = \frac{1}{t_{cycle}} \tag{5}$$

The cycle of a pulse detonation engine can be divided into two main stages: the filling of the tube with combustible gases, and the detonation and exhaust of the products in the atmosphere.

$$t_{cycle} = t_{fill} + t_{detonation} + t_{exhaust} \tag{6}$$

Calculations by Wintenberger et al. (2000) on the impulse of a single-cycle pulse detonation engine have shown that a reasonable time for the combined detonation and exhaust

portion is equal to $10t_{CJ}$, where t_{CJ} is the time taken by the detonation wave to propagate along the tube ($t_{CJ} = L/U_{CJ}$, where U_{CJ} is the Chapman-Jouguet detonation propagation velocity). The impulse is usually maximized after this time, which corresponds to the beginning of a negative overpressure at the thrust wall that decreases the total impulse. The filling time can be very crudely estimated by assuming a constant fill velocity in the tube. This velocity U_{fill} is assumed to be subsonic. The estimate for the filling time is then: $t_{fill} = L/U_{fill}$. The calculations were carried out with two different values of U_{fill}, 100 and 200 m/s. Both of these values have been selected arbitrarily for the purpose of the present analysis. For a tube of a given length, the filling time and the detonation time can be calculated and the maximum repetition frequency determined as

$$f_{max} = \frac{1}{L} \cdot \frac{1}{\frac{10}{U_{CJ}} + \frac{1}{U_{fill}}} \tag{7}$$

As indicated, the maximum repetition frequency will scale inversely with the tube length. The value of the Chapman-Jouguet detonation velocity for stoichiometric JP10–air at P_1=100 kPa and T_1=300 K is: U_{CJ}=1783.5 m/s.

The upper limit for the cycle frequency is shown in Figure 4 for the two different filling velocities. The maximum frequency obviously decreases when the tube length increases because there is more gas to fill and more gas to exhaust. The estimate of the maximum frequency is very crude and idealized, since no other characteristic time has been taken into account than for filling and detonating/exhausting the gases but it gives at least an idea of the magnitude of the frequencies the engine can be operated at. For example, a 1 m-long tube cannot be operated at a frequency over 100 Hz.

2.5 Detonation-related limits

No condition for steady and reproducible detonation propagation has been considered in the design up to now. However, there are limits associated with the detonation parameters of the mixture considered. The key limiting parameter of the mixture is the cell size λ, which is about 60 mm for stoichiometric JP10–air at P_1=100 kPa and T_1=300 K. The cell size is one of the most critical factors to consider when selecting tube diameter. A detonation typically cannot propagate in a tube of diameter less than the cell size divided by π, the limit corresponding to highly unstable or "spinning" detonations. This corresponds to a minimum diameter of about 0.75 inch. A more realistic limit is associated with transition to detonation, which usually requires that the minimum tube size is about one cell width which equals about 2.4 inch. Another constraint on the design is that the tube should be long enough so that the detonation has the time to be successfully initiated. This is especially true if the detonation is created by deflagration-to-detonation transition (DDT). A rough estimate of the minimum length required for detonation initiation and stabilization is 10λ or 23.6 inch.

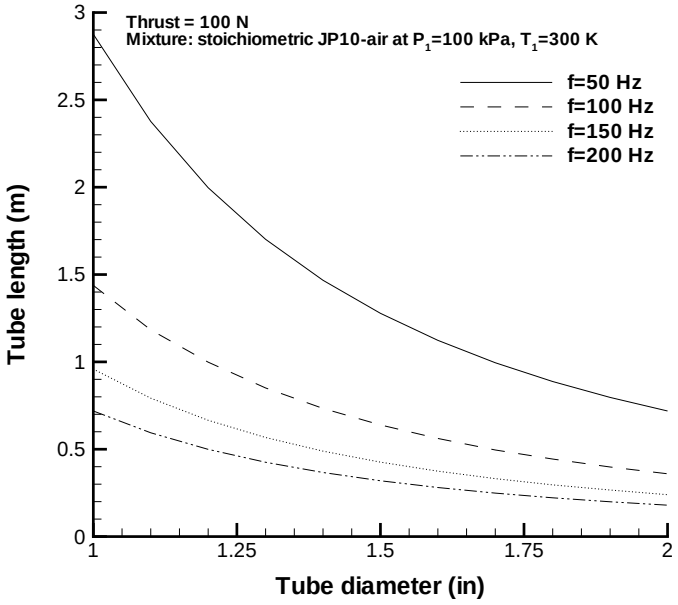

Figure 3: Tube length of a 100 N-thrust JP10–air PDE as a function of tube diameter for different cycle frequencies. Fill conditions of 100 kPa and 300 K.

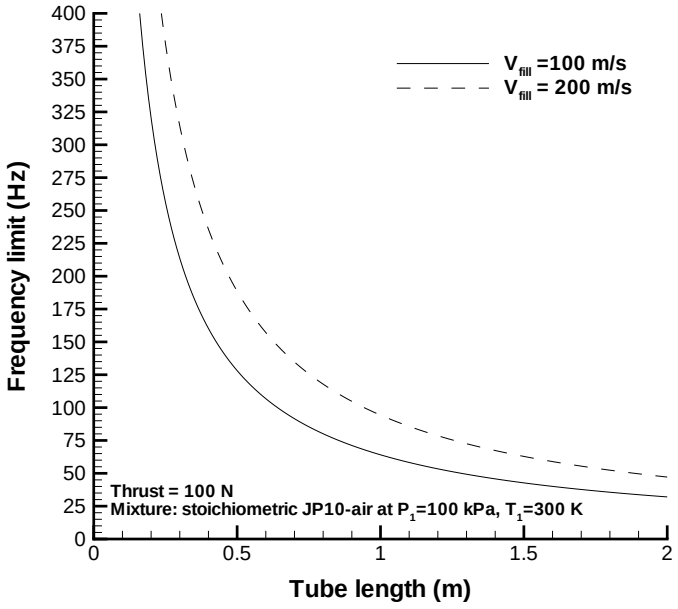

Figure 4: Upper limit to the cycle frequency of a JP10–air PDE as a function of tube length. Fill conditions of 100 kPa and 300 K.

2.6 Three-dimensional design surface

All the limitations discussed in the previous sections must be considered together in order to study the design possibilities in a three-dimensional parameter space including the following variables: tube diameter d, cycle frequency f, and tube length L. These three design parameters are subject to three constraints. The first constraint is the design goal of a fixed thrust, see Eq. 3, which implies that

$$L \propto \frac{1}{d^2} \tag{8}$$

The second constraint is the maximum repetition frequency limit, Eq. 7, which implies that

$$f \leq f_{max} \propto \frac{1}{L} \tag{9}$$

The third constraint is that the tube size must be larger than minimum dimensions which are proportional to the cell width

$$d \geq \lambda/\pi \tag{10}$$

$$L \geq 10\lambda \tag{11}$$

When all of these constraints are considered, only certain combinations of frequency, length, and diameter are possible. We can visualize this by plotting the relationship $f = f(L, d)$ as a surface in the (f, d, L) design space, shown in Figure 5. Note that the various limiting factors are indicated on the boundary of the design surface. The maximum frequency constraint, Eq. 9, limits the minimum tube diameter to greater than 1.25 inch so that the cell width limitation, Eq. 10, does not come into play. The lower limit on the tube length is determined by the DDT criterion, Eq. 11. The other boundaries are determined by the constant thrust design constraint, Eq. 8. A closer view of the design surface is presented in Figure 6. The range of lengths considered goes up to 2 m, which is probably a reasonable upper limit for practical applications. The value of U_{fill} used in constructing these surfaces was 200 m/s.

2.7 Performance design issues

The calculations carried out in this analysis are crude, but nevertheless provide significant insight into the critical issues in the design of a pulse detonation engine. Based on these considerations, we can identify several issues that need further consideration.

2.7.1 Upper frequency limit

The upper frequency limit is associated with a minimum cycle time, which is a function of a detonation and exhaust time and a filling time. For the range of filling velocities examined in the present study, the filling time is comparable to the combined detonation and exhaust time. It must also be noted that unless the mixture is premixed, there will be

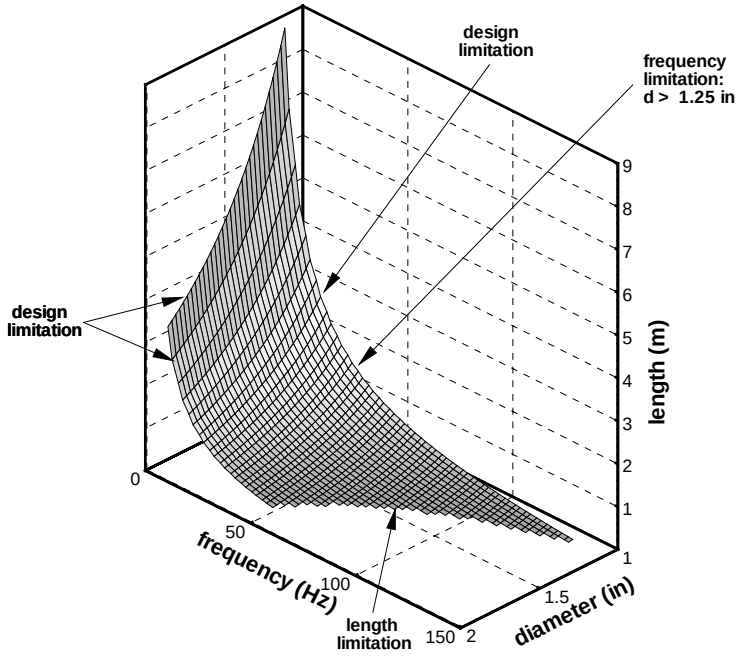

Figure 5: Three-dimensional design surface showing the possible values of the frequency, length, and diameter parameters. Design based on a 100 N JP10-air PDE. Fill conditions of 100 kPa and 300 K, $U_{fill} = 200$ m/s.

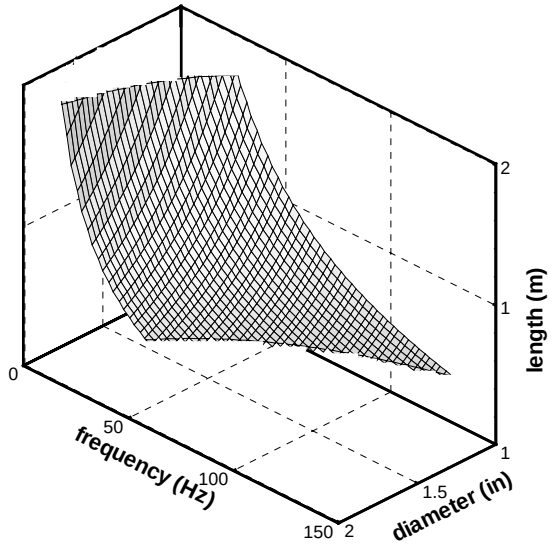

Figure 6: Three-dimensional design surface for a range of tube lengths suitable for practical applications.

a characteristic time associated with mixing, which may increase further the filling time. Practical consideration may also require the introduction of a buffer zone of inert gas (air) to prevent the hot detonation products of the previous cycle from igniting the fresh fuel-air mixture. This would also increase the filling time. We conclude that we have rather unreliable estimates for the filling time and this introduces significant uncertainty into our design estimates.

2.7.2 Detonation sensitivity

The customary measure of detonation sensitivity is the cell width. In our analysis, this is one of the constraints that determines the minimum tube length. Our estimate of the required tube length is rather rudimentary so that the minimum length of the tube is uncertain. Experiments to date in our laboratory have shown that with a careful igniter design, it is possible to initiate a mixture with sensitivity (stoichiometric propane-air, $\lambda = 55$ mm) comparable to JP10–air and obtain nearly ideal performance with a tube diameter of 3 in and length of 40 in. These dimensions are substantially larger than the minimum dimensions used in the present design. If the sensitivity of the mixture could be increased, i.e., the cell width decreased, then the pulse detonation engine could be shorter and run at a higher frequency. This could be achieved by either using a different, more sensitive mixture, or by sensitizing the initial JP10–air mixture.

2.8 Initiation

The important issue of initiation has not been considered at all in the present study. Experience with similar mixtures indicates that deflagration-to-detonation transition (DDT) is not a practical initiation mechanism for short tubes and other techniques will be required. One of the most common approaches considered today is to use a separate chamber in which a detonation is easily initiated by DDT in a much more sensitive fuel-oxygen mixture. This requires carrying a separate supply of oxygen, additional valves, and a control system for the initiator chamber. The coupling of the initiator chamber to the main tube also needs to be addressed. Initiation methods that may eliminate using oxygen are also under consideration; these include shock focusing and hot gas jets.

2.9 Liquid fuels

We have not considered that JP10 is a liquid at room temperature rather than a gas (JP10 has a boiling point of 190°C). Special consideration must be given to fuel atomization and mixing if this is the case in the actual engine. Droplet sizes less than 10 μm will be required in order to avoid substantial decreases in the detonation sensitivity. In actual practice, the engine will be running hot after a short period of operation and there is sufficient waste heat available to warm up the JP10 so that it will completely vaporize upon injection. Operation with commodity fuels such as Jet A will require similar considerations but even higher temperatures may be required to completely vaporize the heavier components.

2.10 Multi-cycle operation

Our design has considered only the factors associated with a single cycle of operation. Repetitive operation will require additional timing considerations, features such as buffer gases, and could significantly impact the design space estimate we have made.

2.11 Drag and flow losses

One of the most obvious omissions from the present study is consideration of the losses associated with the drag on a moving engine and also the flow through the engine during the filling, detonation, and exhaust processes. In order to estimate these losses, we would have to consider a much more sophisticated design that includes an inlet diffuser, bypass geometry, PDE air valve, and exit nozzle. This is clearly essential to realistic engine performance estimates. However, we felt it was not possible for us to include these considerations at the present stage of our experience. There has been no standardization of the engine components and geometry as there has for gas turbines and rockets. In addition, it is unlikely that a simple quasi-one-dimensional steady-flow analysis will be adequate and much more sophisticated computations will be required compared to those that are currently used for gas turbine or rocket motor conceptual design.

2.12 Fill conditions and operational envelope

We have considered only fill conditions that correspond to nominal sea level air. In actual practice, the engine will be on a vehicle moving at a substantial velocity (possibly supersonic) through the atmosphere at some altitude above sea level. Given an inlet diffuser and a flight envelope (velocity-altitude trajectory), it would be possible to compute the effect on the design parameters. By carrying out a series of design space computations at various points in the flight envelope, it would be possible to determine if there existed overlapping parameter ranges that would enable the engine to operate at the design thrust throughout this envelope.

3 Structural considerations

An important aspect of performance is the engine weight; the traditional figure of merit being the thrust-to-weight ratio. The weight will be determined by the choice of material and the wall thickness since the length and diameter are fixed by the performance considerations. To do this, it is necessary to consider the structural design including choice of material, design basis structural loading, transient thermal and stress loading effects associated with the detonation, and the repetitive nature of the loading.

While in a conventional jet engine the main source of stress is the centrifugal force of the rotating parts, in a pulse detonation engine the main stress is the dynamic hoop stress on the cylindrical engine wall. Since the detonation load is highly impulsive and repeti-

tive, the allowable stress will be several times smaller than that obtained by conventional static analysis.

The choice of structural material must account for the environment and the required durability. Many material properties must be known before confidence can be placed in the design. These properties include hardness, tensile and compressive strengths, Young's Modulus, Poisson's ratio, creep rates, oxidation and corrosion rates, fatigue strength, and fatigue crack propagation rate (all as a function of time, temperature, and heat treatment). A substantial amount of information for choosing aircraft engine material is available in the open literature (such as *The Aerospace Structural Metals Handbook*). However, the properties listed are mostly for conventional static loading. A new set of properties for thermomechanically impulsive loading must be compiled for future pulse detonation engine designs.

In the present study, we have considered four representative materials: silicon nitride (Si_3N_4, 6061T6 aluminum , 4340 steel, and Inconel 718). Some room temperature properties of these materials are given in Table 3. Silicon nitride is potentially of interest because of its high strength-to-weight ratio and high temperature properties; however, it has low fracture toughness. Aluminum is a typical aerospace construction material and is widely used in prototype engines; however, it has poor high temperature properties. 4340 steel is a tough steel that is widely used in pressure vessel applications. Inconel 718 is a high temperature material that is widely used in gas turbine construction.

3.1 Geometry

The only engine geometry considered in this report will be cylindrical. In an actual engine, stress concentrations due to geometric changes must be considered. Stress concentrations can easily triple the elastic stress level unless yielding takes place. Features causing stress concentrations include holes, slots, inside and outside corners, interfaces between coatings and parent materials, machine marks, and, the worst of all, cracks. For example, the maximum stress concentration around the edge of a hole is 3 times the nominal hoop stress according to linear elastic theory. Stress concentrations around cracks are even higher, and they are treated in Section 3.4.

3.2 Yield stress criteria

The maximum principle stress on an internally pressurized thin-walled cylinder is the hoop stress σ_H. One of the key design constaints for a tube to withstand an internal detonation pressure is to limit the dynamic hoop stress at a certain safety factor below the tensile yield stress of the material, ensuring that no permanent plastic deformation develops. The maximum dynamic hoop stress constraint can be expressed as

$$\sigma_H = \Phi \frac{\Delta P_{CJ} R}{t} \leq \frac{\sigma_Y}{SF} \tag{12}$$

where σ_Y is the tensile yield stress of the tube material, SF is the safety factor, σ_H is the amplitude of the dynamic hoop stress, Φ is the dynamic amplification factor, ΔP_{CJ}

= P_{CJ} - $P_\circ$, P_{CJ} is the Chapman-Jouguet pressure, $P_\circ$ is the ambient pressure external to the tube, R is the tube mean radius, and t is the wall thickness. Note that $\Delta P_{CJ} R/t$ is the usual static strength of materials estimation of the hoop stress. Since the internal pressure is dynamic, a 'dynamic amplification factor' Φ has to multiply the static hoop stress to obtain the dynamic hoop stress. The dynamic load factor ($1 \leq \Phi \leq 4$) is a function of the detonation wave velocity and will be discussed further in Section 3.3. If the material, safety factor, and mixture are selected, then the remaining variables are the tube radius and wall thickness. Figure 7 shows the minimum wall thickness required for an '$SF = 3$' design of a tube closed at the ignition end and open at the exhaust end. Further, we assume that there is no reflected shock wave and that there are no holes or flaws on the tube.

Once a material is selected (so that σ_Y is fixed), then Eq. 12 implies that the tube thickness has to scale with the radius

$$R \propto t \tag{13}$$

The design criterion of a specified thrust (impulse), Eq. 8, then implies that the thickness has to decrease as the length L increases according to

$$t \propto \frac{1}{\sqrt{fL}} \tag{14}$$

As discussed below, the constraint, Eq. 12, also implies that the thrust-to-weight ratio is proportional to the ratio $f\sigma_Y/\rho$. Maximizing the thrust-to-weight ratio at a fixed repetition frequency corresponds to maximizing σ_Y/ρ. This is known as yield-limited design and is the standard design principle for pressure vessels of minimum weight.

3.3 Structural resonance due to flexural wave excitation

Structural resonance due to flexural wave excitation by detonation loading is similar to airfoil or disk flutter in a conventional jet engine in the sense that they are all fluid-structural interaction phenomena in which resonating stresses are built up by a driving energy extracted from the flowing gas. Structural resonance was analyzed theoretically, numerically, and experimentally by Beltman and Shepherd (1998). The behavior of the structure can be governed by three regimes:

$$U_{CJ} < v_{crit} \qquad \Phi \to 1 \qquad \text{subcritical} \tag{15}$$

$$U_{CJ} = v_{crit} \qquad \Phi \to \infty \qquad \text{critical} \tag{16}$$

$$U_{CJ} > v_{crit} \qquad \Phi \to 2 \qquad \text{supercritical} \tag{17}$$

where U_{CJ} is the Chapman-Jouguet detonation wave speed, v_{crit} is the critical flexural wave speed of the tube, and Φ is the dynamic amplification factor introduced earlier. In reality, due to the finite length of the tube, material yielding, non-linearities, etc., Φ will not be unbounded even if the CJ wave speed is critical. Experiments done by Beltman

and Shepherd (1998) have shown that Φ can be as high as 4. Plots of the critical flexural wave speeds are shown in Figures 8 to 10. Formulas for estimating the critical flexural wave speed of the tube are given in Appendix A.

3.4 Fracture toughness

Fracture mechanics concepts can be used to achieve fracture safety and fracture surveillance of costly structures. The theory assumes the presence of an initial flaw in a body under certain loading, which may or may not be critical. Since no analytical model has been found on the fracture response of a surface-flawed tube to detonation loading, static linear elastic fracture mechanics is assumed here. The simplest model approximates the tube with an axial crack $2a$ in length with a center-cracked plate loaded uniaxially with the hoop stress in mode I. The stress intensity factor K_I of a center-cracked plate loaded by a far field stress σ is:

$$K_I = \sigma\sqrt{(\pi a)} \tag{18}$$

In this case, σ is substituted by the dynamic hoop stress of a cylinder, $\Phi\Delta P_{CJ}R/t$. Fracture is expected to occur when $K_I = K_{Ic}$, where K_{Ic} is the fracture toughness. Figures 11 to 13 show critical crack lengths for different materials and conditions.

3.5 Thrust-to-weight ratio (T/W)

The weight of the tube[3] is approximately given by

$$W = \rho \cdot t \cdot L \cdot 2\pi R \tag{19}$$

for a thin-wall tube. The thrust-to-weight ratio T/W can be computed using the definition of thrust from Eq. 3

$$T/W = \frac{fI_v}{2g_\circ\rho}\frac{R}{t} \tag{20}$$

This can be simplified by using the yield-limited design criterion, Eq. 12, to eliminate R/t to obtain

$$T/W = f \cdot \frac{\sigma_Y}{\rho} \cdot \frac{I_v}{\Delta P_{CJ}} \cdot \frac{1}{\Phi SF g_\circ} \tag{21}$$

Note that the impulse per unit volume is proportional to ΔP_{CJ} so that for all other factors being held constant, we have

$$T/W \propto f\frac{\sigma_Y}{\rho} \tag{22}$$

The densities of the materials chosen for comparison are listed in Table 3. Plots of thrust-to-weight ratios for different conditions are shown from Figures 14 to 16. The

[3]Note that this is not the total engine weight since we have not included any of the other components such as the inlet, valves, exit nozzle, etc. For a true measure of the viability of an engine concept in comparison to existing engines, it will be important to consider these factors.

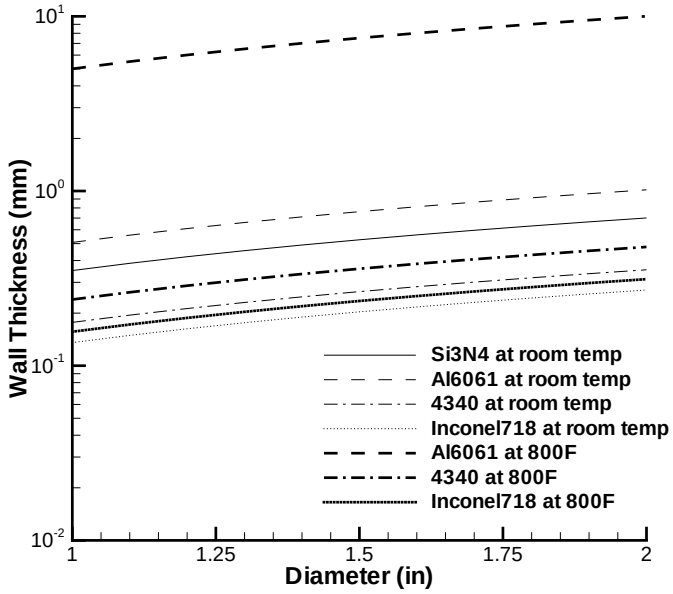

Figure 7: Minimum wall thickness required using the yield stress design and a safety factor of 3. JP10-air PDE design.

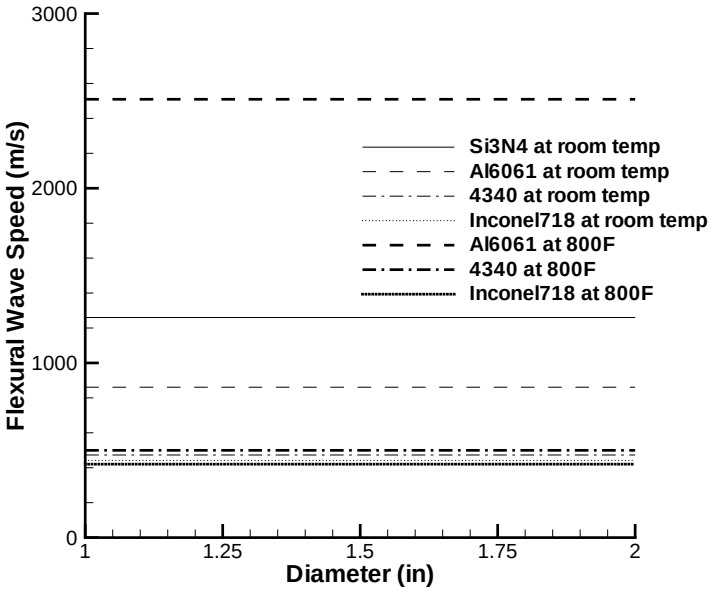

Figure 8: Critical flexural wave speed of the cylinder designed by using the yield stress criteria and a safety factor of 3. The Chapman-Jouguet wave speed in this study is 1784 m/s.

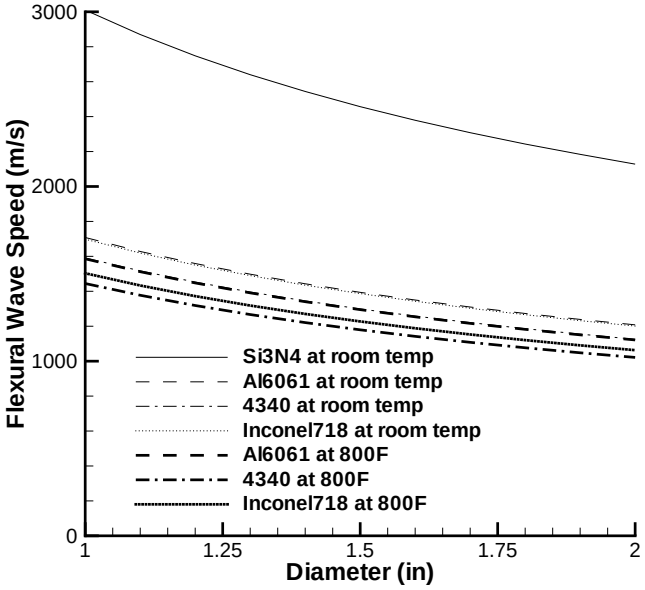

Figure 9: Critical flexural wave speed of the cylinder designed by fixing the wall thickness at 2 mm. The Chapman-Jouguet wave speed in this study is 1784 m/s.

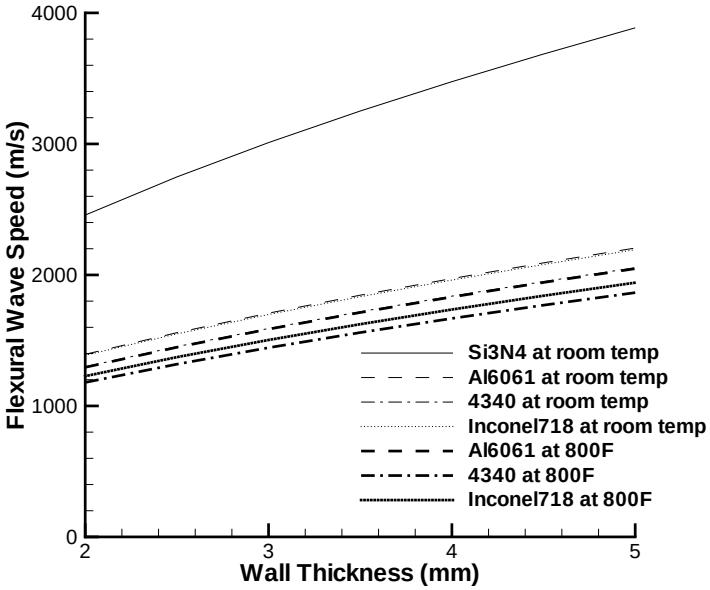

Figure 10: Critical flexural wave speed of the cylinder designed by fixing the tube diameter at 1.5 inches. The Chapman-Jouguet wave speed in this study is 1784 m/s.

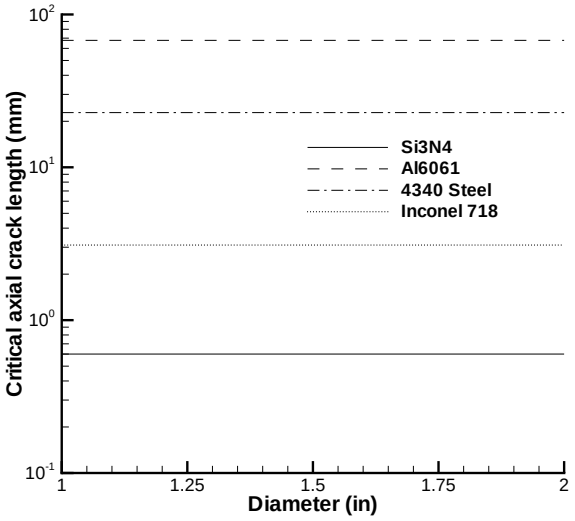

Figure 11: Critical through-the-wall-thickness axial crack length of the cylinder designed by using the yield stress criteria and a safety factor of 3. Static linear elastic fracture mechanics and room temperature are assumed.

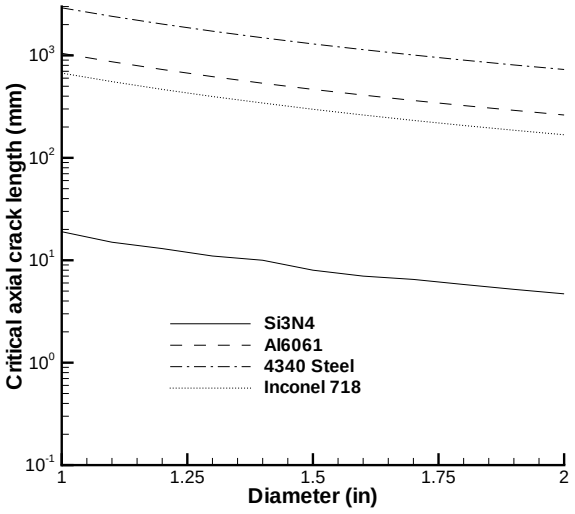

Figure 12: Critical through-the-wall-thickness axial crack length of the cylinder designed by fixing the wall thickness at 2 mm. Static linear elastic fracture mechanics and room temperature are assumed.

tube weight is a function of the tube length, which is a function of the cycling frequency (discussed in the performance section). There are pairs of curves that are so close together they become virtually indistinguishable on the figures. These include: the aluminum and steel curves on Figure 14 and the steel and inconel curves on Figures 15 and 16. Note also that for the fixed wall thickness (2 mm) and fixed tube diameter (1.5 inches) designs, steel and inconel engines become too heavy (engine mass > 1.2 kg) for part of the range of variables considered.

Material	ρ (kg/m^3)	σ_Y (MPa)	E (GPa)	K_{Ic} (MPa·m^2)	ν	σ_Y/ρ (MPa·m^3/kg)
Silicon Nitride	3500	400	304	4	0.24	0.114
4340 Steel	8000	792	193	50	0.25	0.099
Aluminum	2780	276	73	30	0.33	0.099
Inconel 718	8100	1034	215	24	0.30	0.127

Table 3: Properties of four materials at room temperature.

3.6 Structural design issues

3.6.1 Impulsive thermomechanical fatigue

Two types of fatigue are of major concern to PDEs. The first is mechanical fatigue, which is caused by the fluctuations in the stresses due to the repetitive detonation pressure loads. The second is thermal fatigue, which is caused by thermal stresses, environmental interaction (oxidation), and creep. Thermal stresses can arise in a material if either free expansion or contraction is prevented or if it is heated or cooled in such a way that a thermal stress gradient exists across it. In practice, thermal stresses are seldom large enough to cause static failure, but repeated applications may lead to fatigue failure. When a PDE is run at elevated temperatures, large temperature gradients may develop across the inner wall that is in direct contact with the detonation wave, and the outer wall that is in contact with the coolant. This will cause thermal stress fatigue.

Environmental interaction typically involves the diffusion of oxygen into the region ahead of the crack tip along the grain boundaries. This causes the material to become brittle along these grain boundaries and fracture under the applied stress field. Fracture allows further oxide penetration. Crack growth for this mechanism is a function of the diffusion rate of oxygen ahead of the crack tip and is a time-dependent process that depends on the time of exposure at a given stress level. Creep fatigue, on the other hand, is actuated by high temperatures that are significant fractions of the homologous temperature as the inelastic deformation becomes significant. The mechanisms for fracture caused by creep are time-dependent rather than cycle-dependent. Thermal fatigue and mechanical fatigue couple to induce *thermomechanical fatigue*, and this is one of the most complex topics in materials research. Although micromechanisms, models, and

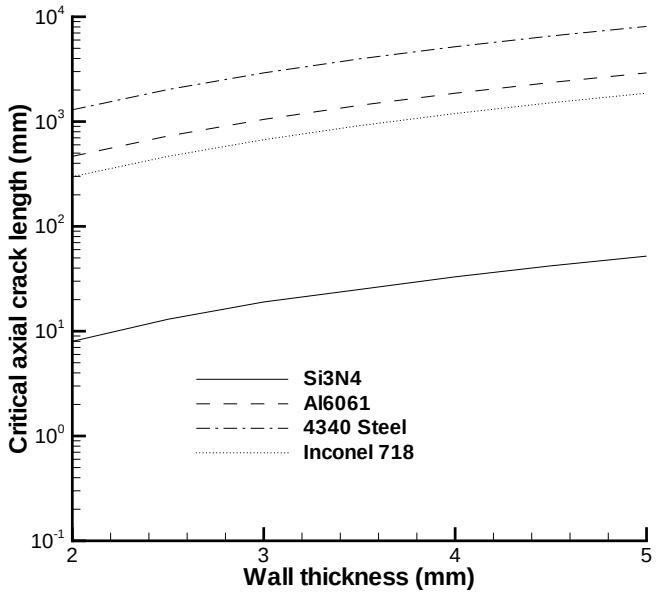

Figure 13: Critical through-the-wall-thickness axial crack length of the cylinder designed by fixing the tube diameter at 1.5 inches. Static linear elastic fracture mechanics and room temperature are assumed.

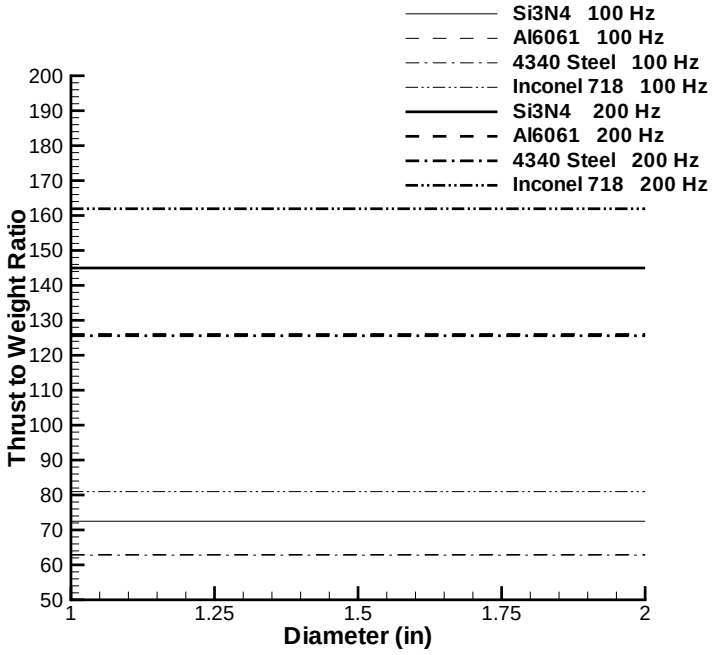

Figure 14: Thrust-to-weight ratio of the engine designed by using the yield stress criteria and a safety factor of 3. Room temperature is assumed.

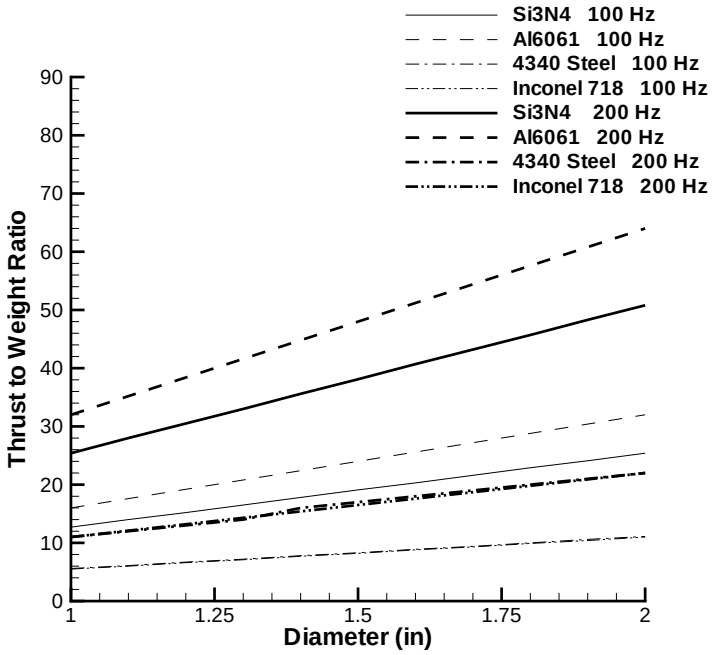

Figure 15: Thrust-to-weight ratio of the engine designed by fixing the wall thickness at 2 mm. Room temperature is assumed.

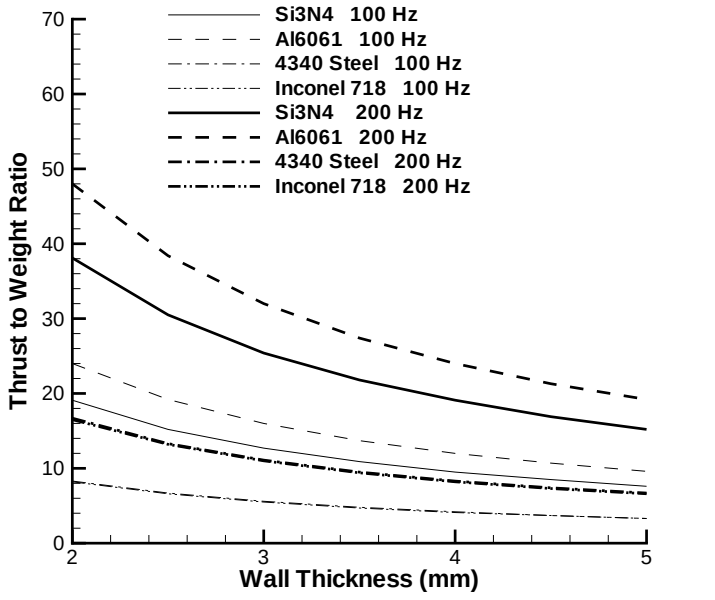

Figure 16: Thrust-to-weight ratio of the engine designed by fixing the tube diameter at 1.5 inches. Room temperature is assumed.

characterization methodology for thermomechanical fatigue crack initiation and growth exist, our current knowledge is far from complete.

3.6.2 Fracture due to single-cycle detonation loading

The fundamental physics of crack initiation, propagation, and arrest due to single-cycle detonation loading is not well understood. The static fracture analysis employed in the section above is crude and there is yet no way to know the associated uncertainty of critical crack size predictions because the behavior of dynamic cracks is very sensitive to the time scales and magnitudes of impulsive loading. Research on fracture response of tubes to single-cycle detonation loading at room temperature is currently under way at Caltech. Preliminary results can be found in Chao and Shepherd (2000).

3.6.3 Plastic creep due to cyclic detonation loading

If a long service time is considered (say, on the order of 1000 hours), traditional yield strength design would not be a conservative design practice because the structure will undergo plastic creep during the exposure time which could cause unacceptable distortion and/or interference. It is preferable to base designs on creep and creep rupture data. Common practice is to allow less than 1% creep during the life of the structure and this may become a more restrictive criterion than the yield stress design. Experiments are needed to determine the creep characteristics of different candidate materials under cyclic detonation loading.

4 Summary

To summarize our results, we have computed the performance and structural parameters for a design that uses a tube of a fixed diameter, 1.5 in. The performance parameters are given in Table 4. The key result of these computations is the margin between the operating repetition frequency and the maximum possible value. This will determine how large an excursion in fill density can be compensated for by varying the repetition frequency. We have examined two lengths to illustrate the effect of tube length on the margin available. Note that when the length of the tube varies, so does the maximum frequency f_{max}, so taking a longer tube does not necessarily mean you have more margin. More detailed computations using a flight profile would be needed to examine this issue in depth.

L(m)	f(Hz)	f_{max}(Hz)
0.6	106	157
1	64	94

Table 4: Performance characteristics for a PDE of diameter 1.5 inch. T=100 N, d=1.5 in, V_{fill}=200 m/s

The structural parameters are calculated for a design point of 1.5 inches in diameter. They are summarized in table 5 that shows values obtained from the yield stress criterion, and table 6 that shows values obtained by fixing the wall thickness at 2 mm. The material properties are all in room temperature. The main tradeoff is between the thrust-to-weight ratio and the critical crack length. If one designs according to the yield stress criterion, aluminum and steel will have poorer thrust-to-weight ratios but excellent critical crack lengths. This means that catastrophic structural failure is unlikely. Silicon nitride has a higher thrust-to-weight ratio, but it is the most susceptible amongst the four materials to small flaws. In the case of silicon nitride, keeping the hoop stress at a safety factor below the yield stress is not sufficient. The critical crack length has become a more critical design constraint. Walls must be made much thicker than the minimum wall thickness required by the yield stress criterion so that a potential crack may grow long enough to be inspected before it causes catastrophic failure.

It must be emphasized again that the calculations made here are not for the typical elevated temperatures that a PDE must experience. The fracture mechanics employed here are only static estimations. Only one of the four materials examined above, inconel 718, is commonly used in aircraft engines. Further research must be carried out to find the right material and structural parameters for an operating PDE. *The Aerospace Structural Metals Handbook* is a useful starting place in choosing candidate materials.

Material	*Wall thickness (mm)*	*Flexural wave speed(m/s)*	*Critical crack length(mm)*	*T/W*	
				f=106Hz L=0.6m	*f=64Hz L=1.0m*
Silicon Nitride	0.53	1260	0.6	76	46
Al6061-T6	0.76	861	67.7	67	40
4340 Steel	0.27	473	22.8	67	40
Inconel718	0.20	442	3.1	86	52

Table 5: Structural parameters for a PDE that is 1.5 in in diameter. The yield stress criterion with a safety factor of 3 is used. The wall thickness calculated here is only a lower bound. The other parameters are calculated according to this minimum required wall thickness.

Material	*Wall thickness (mm)*	*Flexural wave speed(m/s)*	*Critical crack length(mm)*	*T/W*	
				f=106Hz L=0.6m	*f=64Hz L=1.0m*
Silicon Nitride	2	2457	8	20	12
Al6061-T6	2	1394	466	25	15
4340 Steel	2	1299	1295	9	5
Inconel718	2	1387	298	9	5

Table 6: Structural parameters for a PDE that is 1.5 in in diameter. The wall thickness is fixed at 2 mm.

References

Beltman, W. M. and J. E. Shepherd (1998). Structural response of shells to detonation and shock loading. GALCIT Report, Graduate Aeronautical Laboratories, California Institute of Technology.

Chao, T. W. and J. E. Shepherd (2000). Fracture response of tubes to detonation loading: Preliminary results. GALCIT Report FM00-9, Graduate Aeronautical Laboratories, California Institute of Technology.

Hill, P. G. and C. R. Peterson (1992). *Mechanics and Thermodynamics of Propulsion* (Second ed.). Addison-Wesley.

Mattingly, J. D., W. H. Heiser, and D. H. Daley (1987). *Aircraft Engine Design* (Second ed.). American Institute of Aeronautics and Astronautics.

Suresh, S. (1991). *Fatigue of Materials*. Cambridge University Press.

Wintenberger, E., J. Austin, M. Cooper, S. Jackson, and J. E. Shepherd (2000). Impulse of a single-cycle pulse detonation engine. GALCIT Report FM00-8, Graduate Aeronautical Laboratories, California Institute of Technology.

A Critical flexural wave speed

The formulas in this section are taken from Beltman and Shepherd (1998) and can be used to compute the critical flexural wave speed under detonation or shock loading conditions in a thin-wall tube. Two estimates are given, both are for the case of a steady-state (infinite length) thin-walled tube. The first case included the effect of shear and rotary inertia, the second case neglects these effects. The second case is much simpler to apply and is useful to get a first estimate of the critical flexural wave speed.

With shear and rotary inertia

Assumptions:

- rotary symmetry
- tube of infinite length
- linear elastic material
- no axial prestress
- thin wall compared to radius

To get v, the flexural wave speed, solve the dispersion equation

$$A_2^2 - 4A_0A_4 = 0 \tag{23}$$

where

$$A_0 = \beta^2 \left(1 + \frac{\nu^2}{\left(\frac{v}{v_d}\right)^2 - 1} \right) \tag{24}$$

$$A_2 = \left(\frac{v}{v_d}\right)^2 \left(1 + \beta^2 \left(\frac{v_d}{v_s}\right)^2\right) - \beta^2(1-\nu^2)\left(\frac{v_d}{v_s}\right)^2 \tag{25}$$

$$A_4 = \left(\left(\frac{v}{v_d}\right)^2 - 1\right)\left(\left(\frac{v}{v_s}\right)^2 - 1\right) \tag{26}$$

$$\begin{aligned} v_d &= \sqrt{\frac{E}{\rho\,(1-\nu^2)}} && \text{: dilatational wave velocity} \\ v_s &= \sqrt{\frac{\kappa G}{\rho}} && \text{: modified shear wave velocity} \\ \beta &= \frac{t}{\sqrt{12}R} && \text{: shell thickness parameter} \end{aligned} \tag{27}$$

where E is the Young's modulus, ρ is the material density, G is the shear modulus, t is the wall thickness, R is the tube radius, and ν is the Poisson's ratio. κ is the shear correction factor evaluated by solving:

$$\sqrt{(n^2-\kappa)(1-\kappa)} = n(\frac{1}{2}\kappa - 1)^2 \tag{28}$$

where

$$n = \sqrt{\frac{2(1-\nu)}{1-2\nu}} \tag{29}$$

Note that for $0 < \nu < 0.5$, the value of κ must be selected so that $0.76 < \kappa < 0.91$.

Without shear and rotary inertia

Assumptions:

- rotary symmetry
- tube of infinite length
- linear elastic material
- no axial prestress
- no shear deformation
- no rotary inertia
- thin wall compared to radius

The flexural wave speed is then

$$v = \left(\frac{E^2 t^2}{3\rho^2 R^2 (1-\nu^2)}\right)^{\frac{1}{4}} \tag{30}$$